

Cite this: *J. Mater. Chem. A*, 2021, 9, 11312

Sulfur-stabilised copper nanoparticles for the aerobic oxidation of amines to imines under ambient conditions†

Iris Martín-García, Gloria Díaz-Reyes,  George Sloan, ‡ Yanina Moglie  § and Francisco Alonso  *

The stabilisation of metal nanoparticles and control of their oxidation state are crucial factors in nanocatalysis. Elemental sulfur has been found to be a cheap and effective stabilising agent for copper nanoparticles in the form of copper(I) oxide. The Cu₂ONPs/S₈ system has been characterised by ICP-OES, EDX, XRD, XPS, FE-SEM, SEM, TEM and Cryo-EM. Astonishingly, in organic medium, the copper nanoparticles are organised as concentric rings within nanodroplets of sulfur of ca. 20–70 nm. In synthetic organic chemistry, imines can be directly obtained by the less studied and practiced oxidation of primary amines; however, the reaction conditions utilised are usually harsh and far from meeting the principles of Green Chemistry. Cu₂ONPs/S₈ has been successfully applied to the solvent-free aerobic oxidation of primary amines to imines under ambient conditions, using air as a terminal oxidant. The catalyst is effective in the homo- and heterocoupling of benzylic amines at very low copper loading (0.3 mol%), being catalytically superior to a range of commercial copper catalysts. A reaction mechanism has been proposed based on experimental evidence, which clarifies the major uncertainty regarding the key intermediate. The results of this study suggest a number of new avenues for research in nanocatalysis.

Received 31st December 2020
Accepted 13th April 2021

DOI: 10.1039/d0ta12621g

rsc.li/materials-a

Introduction

Nanocatalysis has experienced a vertiginous growth in the last two decades.¹ In particular, the development of selective and efficient transition metal nanoparticles (NPs) represents a key area in catalyst development.² These NPs often exhibit superior catalytic activity to their bulk metal counterparts, derived from their high specific surface area and abundance of active catalytic sites.³ Therefore, research into their potential applications can lead to the discovery of new catalytic routes or the improvement of existing catalytic activities and selectivities. However, NPs are susceptible to agglomeration into larger clusters during their synthesis, use as catalysts and/or when stored over time. This phenomenon normally curtails the catalytic activity of the NPs but can be prevented by the use of

stabilising agents, which achieve a larger inter-particle separation by electrostatic, steric or electrosteric interactions.^{1b} Although the application of stabilising agents for NPs and their role is quite well established, research on novel effective and inexpensive anti-agglomeration agents is welcome.

Copper occupies a privileged position within the realm of transition metals because copper is relatively earth-abundant, cheap, has low toxicity and is catalytically active in its different oxidation states. That is why, in the context of nanocatalysis, copper nanoparticles (CuNPs) are a competitive alternative to the more expensive precious transition metal nanoparticles and have gained ground, for instance, on PdNPs in multiple organic transformations.⁴ Although bulk copper-catalysed organic reactions have been widely practiced under aerobic conditions,⁵ the application of CuNPs in air is more limited because of their tendency to undergo uncontrolled oxidation.⁶ Therefore, it is challenging to develop catalytic systems based on CuNPs, where Cu is in a neat lower oxidation state [*i.e.*, Cu(0) or Cu(I)] and resistant to oxidation over time.⁷

Elemental sulfur is produced as a by-product during the hydrodesulfurisation of crude oil and natural gas. It has limited applications as a reactant, beyond the production of sulphuric acid, though is an economic, simple and versatile reagent and promoter in multiple organic transformations.⁸ Its application in materials science has received comparatively little attention, with most contributions published during the last decade.⁹ The introduction of elemental sulfur as a tool to develop metal

Instituto de Síntesis Orgánica and Departamento de Química Orgánica, Facultad de Ciencias, Universidad de Alicante, Apdo. 99, 03080 Alicante, Spain. E-mail: falonso@ua.es

† Electronic supplementary information (ESI) available: General, synthetic procedures, compound characterisation, NMR, XPS, Auger and XRD spectra, EM micrographs, physisorption and droplet-size distribution graphics. See DOI: 10.1039/d0ta12621g

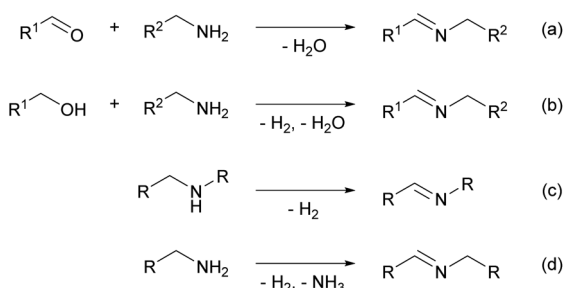
‡ Visiting Erasmus student at the University of Alicante. On leave from the University of Edinburg, United Kingdom.

§ Present address: Departamento de Química Orgánica, INQUISUR, Universidad Nacional del Sur (UNS)-CONICET, Avenida Alem 1253, Bahía Blanca, 8000, Argentina.

nanoparticles with novel or improved properties is barely documented, noteworthy exception being its use as a novel medium to synthesise isolated ligand-capped AuNPs or a vulcanised sulfur-AuNPs nanocomposite.¹⁰ Although copper sulfide nanoparticles have been widely studied and applied,¹¹ to the best of our knowledge, the potential use of elemental sulfur to stabilise CuNPs remains unexplored.

Imines (Schiff bases) are versatile organic compounds used as intermediates in the synthesis of nitrogen-containing heterocyclic compounds, as well as building blocks for the synthesis of fine chemicals and pharmaceuticals.¹² Imines can undergo organic transformations through the carbon–nitrogen double bond leading, among others, to the very useful amines.¹³ Many Schiff-based complexes have demonstrated an excellent activity in homogeneous and heterogeneous catalysis.¹⁴ Imines have traditionally been prepared through the condensation of carbonyl compounds and amines (Scheme 1a).¹⁵ In recent years, significant progress has been made in the synthesis of imines with alternative starting materials, using molecular oxygen or air as green terminal oxidants. These new approaches include the oxidative cross dehydrogenation of alcohols and amines (Scheme 1b),¹⁶ the oxidative dehydrogenation of secondary amines (Scheme 1c)¹⁷ and the direct oxidation of primary amines (Scheme 1d).¹⁸

The transformation of primary amines into imines has lately attracted a great deal of attention,¹⁸ achieved variously through transition-metal catalysis using precious (Au,¹⁹ Ru,²⁰ Ir,²¹ *etc.*) and non-precious metals (Cu,²² Co,²³ Mn,²⁴ Fe,²⁵ *etc.*), metal-free²⁶ and photochemical protocols.²⁷ Even though these procedures have proven to be generally effective in this transformation, most of the catalytic systems are sub-optimal from the Green Chemistry viewpoint. For instance: (a) the common harsh conditions (≥ 100 °C) applied under transition-metal catalysis should be replaced by ambient conditions, preferably using low-loading cheap metals; (b) the use of organic solvents (*e.g.*, PhMe, MeCN, THF, MeOH, CHCl₃) should be minimised in favour of solvent-free systems; (c) the catalytic systems should be simplified whenever possible, avoiding the inclusion of bases, ligands, co-oxidants, *etc.*; and (d) aerobic oxidations should be prioritised over the deployment of stoichiometric oxidants. Although the utilisation of molecular oxygen has become widespread in these reactions, the development of catalytic systems based on air that meet the aforementioned guidelines is more challenging.



Scheme 1 Different approaches to the synthesis of imines.

Owing to our interest in developing efficient synthetic methodologies based on transition-metal nanoparticles,²⁸ we present herein the unprecedented stabilising effect of elemental sulfur on CuNPs and their application in the aerobic oxidation of primary amines to imines under ambient conditions.

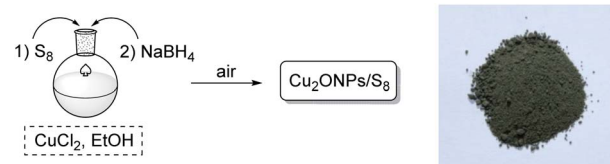
Results and discussion

Optimisation of the catalyst and reaction conditions

In our commitment to search for the optimum catalyst, an initial study was conducted by screening CuNPs on different supports and using the oxidation of benzylamine (**1a**) to (*E*)-*N*-(benzylidene)benzylamine (**2a**) as a model reaction in air as a terminal oxidant. The catalysts were prepared by reduction of anhydrous CuCl₂ with metal lithium in THF under argon, in the presence of 4,4'-di-*tert*-butylbiphenyl as an electron carrier,²⁹ followed by the addition of the support.³⁰ The generation of Cu(0)NPs was evidenced by the formation of black or deep-grey suspensions. All suspensions were subjected to filtration, filtrate washing and drying in air, that is why the resulting materials were obtained in the form of copper oxides.³⁰ In the case of elemental sulfur, the catalyst was obtained by preparing a homogeneous mixture of CuCl₂ in ethanol, followed by the addition of S₈ and reduction with NaBH₄ in air (Scheme 2). Similarly as above, Cu(0)NPs were rapidly formed and the copper–sulfur stuff was subjected to the same work-up protocol in air. In this case, we have noticed that the order of addition of the reagents is important: substantial metal leaching occurs during the washing step if NaBH₄ is added before sulfur, as a sign of the loss of the stabilisation effect apparently exerted by sulfur.

Preliminary experiments with different solvents and reaction temperatures allowed us to settle on room temperature and absence of solvents as the best conditions for comparative purposes (Table 1).

Control assays in the absence of catalyst confirmed the necessity of a catalyst to trigger the reaction (Table 1, entries 1 and 2). Amongst the different catalysts tested, those based on CuNPs on activated carbon, zeolite Y and elemental sulfur gave the best results, with the latter two reaching quantitative conversion (Table 1, entries 3, 6 and 13). It is noteworthy that elemental sulfur alone promoted this transformation, albeit to a lesser extent (Table 1, entries 15–17).³¹ In order to more accurately discern on the suitability of CuNPs/ZY or Cu₂ONPs/S₈, other amines were subjected to the action of both catalysts, with Cu₂ONPs/S₈ showing higher conversions. Therefore, the catalytic system of choice was that consisting of Cu₂ONPs/S₈,



Scheme 2 Preparation scheme and picture of Cu₂ONPs/S₈.

Table 1 Screening of different Cu catalysts in the oxidation of benzylamine (**1a**)^a

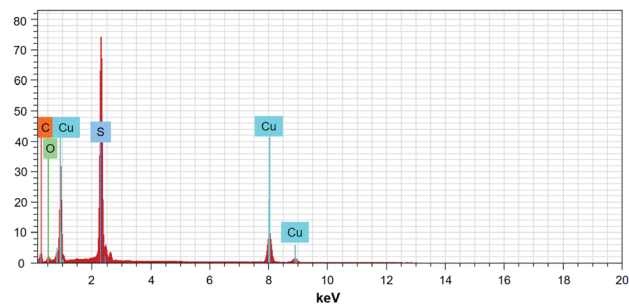
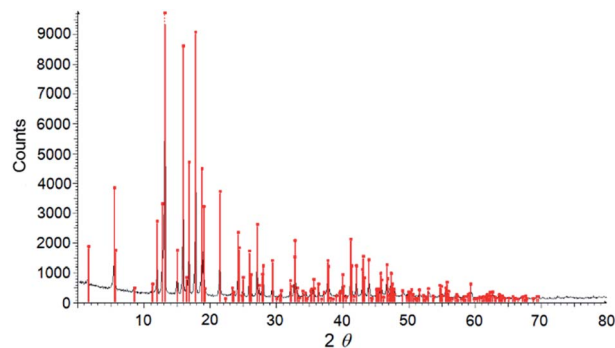
Entry	Catalyst ^b (wt% Cu)	<i>t</i> (h)	Conversion ^c (%)
1	—	24	0
2	—	48 ^d	4
3	CuNPs/C ^e (1.4)	24	89
4	CuNPs/MK-10 ^f (1.8)	24	7
5	CuNPs/MgO (1.5)	24	6
6	CuNPs/ZY^g (3.0)	24	>99
7	CuNPs/Al ₂ O ₃ (2.4)	24	50
8	CuNPs/K ₂ S ₂ O ₈ (2.5)	24	43
9	CuNPs/CeO ₂ (3.7)	24	17
10	CuNPs/ZnO (3.0)	24	30
11	CuNPs/TiO ₂ (3.0)	24	3
12	Cu ₂ ONPs/S ₈ (1.3) ^h	3	68
13	Cu₂ONPs/S₈ (1.3)^h	6	>99
14	Cu ₂ ONPs/S ₈ (1.3) ^h	24	>99
15	S ₈ ^h	3	15
16	S ₈ ^h	6	15
17	S ₈ ^h	24	20

^a Reaction conditions: benzylamine (**1a**, 1 mmol), CuNPs/support (50 mg), neat, rt, air, unless otherwise stated. ^b CuNPs refers to a mixture of Cu₂O and CuO. ^c Conversion into **2a** determined by GLC. ^d Reaction at 70 °C. ^e Activated carbon. ^f Montmorillonite K-10. ^g Zeolite Y. ^h 20 mg.

applied at room temperature under solvent-free conditions in air.

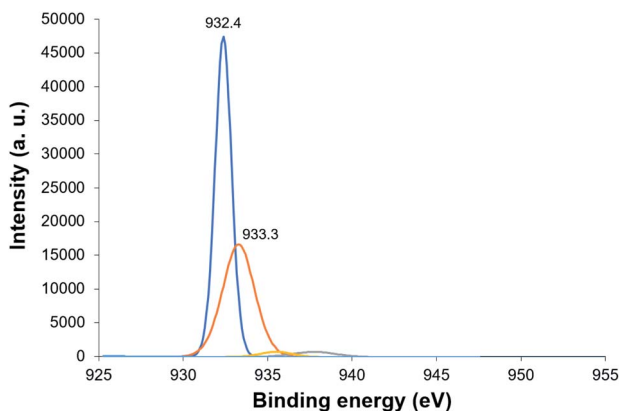
Catalyst characterisation

The catalyst Cu₂ONPs/S₈ was characterised by different analytical and spectroscopic techniques, such as ICP-OES, EDX, XRD, XPS, FE-SEM, SEM, TEM and Cryo-EM. The copper loading on Cu₂ONPs/S₈ was determined to be 1.30 wt%, as analysed by Inductively-Coupled Plasma-Optical Emission Spectroscopy (ICP-OES). The obtained adsorption isotherm (N₂ at 77 K) shows that Cu₂ONPs/S₈ is a material with very low adsorption capacity (Fig. S1†). The isotherm can be classified as a type II or pseudo-type II, with a type-H3 hysteresis loop. This isotherm shape indicates that the sample contains mesopores but not micropores. The shape of the H3 loop is usually linked with the non-rigid nature of the adsorbent.³² In agreement with the low adsorption capacity, the calculated BET surface area is 22.7 m² g⁻¹. A pore volume of 0.085 cm³ g⁻¹ has been estimated by applying the BJH model to the desorption branch data, with an average size of 5.5 nm (although the BJH shows other small relative maxima, they are not significant considering the low pore volume).³² Energy-Dispersive X-ray (EDX) analysis on various regions confirmed the presence of sulfur (K line, 2.31 keV), oxygen (K line, 0.53) and copper, the latter with energy bands of 8.04, 8.90 keV (K lines) and 0.93 keV (L line) (Fig. 1); the presence of carbon is due to the use of a carbon support during the analysis. The estimated superficial atomic distribution by

**Fig. 1** EDX spectrum of Cu₂ONPs/S₈.**Fig. 2** XRD spectrum of Cu₂ONPs/S₈ (■ denotes orthorhombic S).

EDX, Cu (32.3%), O (18.1%) and S (49.6%), gives a Cu/O ratio (1.8) close to that expected for copper in the form of Cu₂O. The examination of Cu₂ONPs/S₈ by powder X-ray Diffraction (XRD) (Fig. 2 and S2†) showed diffraction peaks corresponding to orthorhombic sulfur; no significant peak for copper was observed due to the small crystal domains, low copper loading or high dispersion.

The oxidation state of copper was ascertained by X-ray Photoelectron Spectroscopy (XPS). For a comparative purpose, we also analysed by XPS a sample of recently purchased Cu₂S. The XPS spectrum of Cu₂ONPs/S₈ and Cu₂S at the Cu 2p_{3/2} level look very similar, with peaks at 932.4 and 933.3 eV (Cu₂ONPs/S₈)

**Fig. 3** XPS spectrum at the Cu 2p_{3/2} level of Cu₂ONPs/S₈.

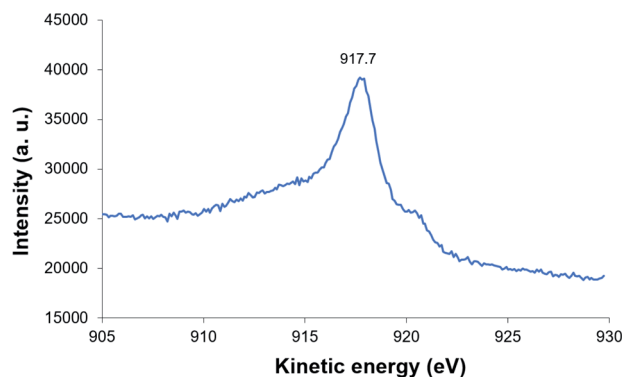


Fig. 4 Auger spectrum of $\text{Cu}_2\text{ONPs/S}_8$ (Cu LMM line).

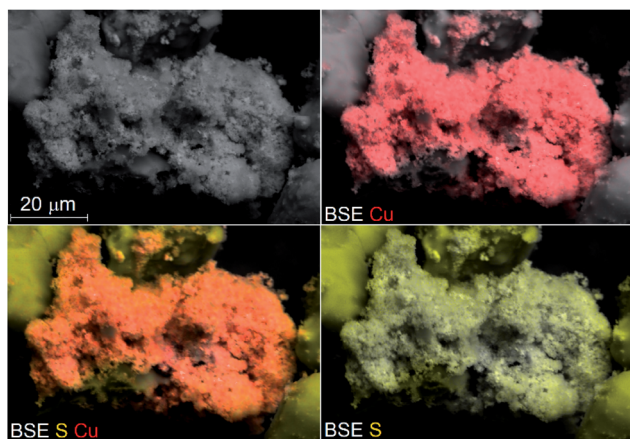


Fig. 5 SEM micrographs and element mapping of $\text{Cu}_2\text{ONPs/S}_8$.

(Fig. 3), and 932.5 and 933.2 eV (Cu_2S) (Fig. S3†).³³ The absence of the satellite peaks in the region 940–945 eV suggests that the catalyst is practically free of Cu^{II} species in the form of CuO .³⁴

Auger spectroscopy on $\text{Cu}_2\text{ONPs/S}_8$ and Cu_2S samples (Cu LMM lines) brought into view very close kinetic energies at 917.7 and 917.5 eV, respectively (Fig. 4 and S3†).³⁵ In contrast, the main binding energies noted at the S $2p_{3/2}$ and S $2p_{1/2}$ levels are very different: 164.4 and 165.6 eV for $\text{Cu}_2\text{ONPs/S}_8$ (typical of elemental sulfur),³³ and 161.7 and 163.1 eV for Cu_2S ³⁵ (Fig. S3†). These data point to the copper in our catalyst being primarily composed of Cu_2O , whereas the formation of Cu_2S during the catalyst preparation can be practically ruled out. Surprisingly, a catalyst sample kept in air for some years barely changed its composition, though the presence of some CuO was visible through its XPS Cu $2p_{3/2}$ peak at 934.9 eV and its two characteristic satellite peaks at 941.4 and 944.3 eV (ESI, Fig. S4†),^{30a} proving the strong stabilising effect of sulfur to prevent further oxidation.

The characterisation of $\text{Cu}_2\text{ONPs/S}_8$ by standard electron microscopy techniques was troublesome. Due to the low melting point of sulfur (115.2 °C), the application of a higher energy incident beam to better observe the contrast between the Cu_2ONPs and sulfur just melt the latter. The morphology of $\text{Cu}_2\text{ONPs/S}_8$ showing the surface texture of sulfur could be observed by FE-SEM and SEM, whereas the superficial analysis by TEM was inconclusive (Fig. S5†). Element mapping by SEM displayed the presence of Cu and S, with a layer of the latter seemingly having a protective effect on Cu (Fig. 5). Cryogenic Electron Microscopy (Cryo-EM)³⁶ was found to be an appropriate technique to observe $\text{Cu}_2\text{ONPs/S}_8$ without sulfur melting (Fig. 6). When $\text{Cu}_2\text{ONPs/S}_8$ was dispersed in an organic medium (e.g., ethanol), circular droplets were brought into view with a size range of ca. 20–70 nm (median = 47 nm) (ESI, Fig. S6†). The droplets contained a nearly concentric ring distribution of the Cu_2ONPs with respect to the droplet surfaces, which were themselves surrounded by sulfur (Fig. 6c–f). The general insolubility of sulfur could account for this particular arrangement of the nanoparticles inside the droplet. Apparently, sulfur acts

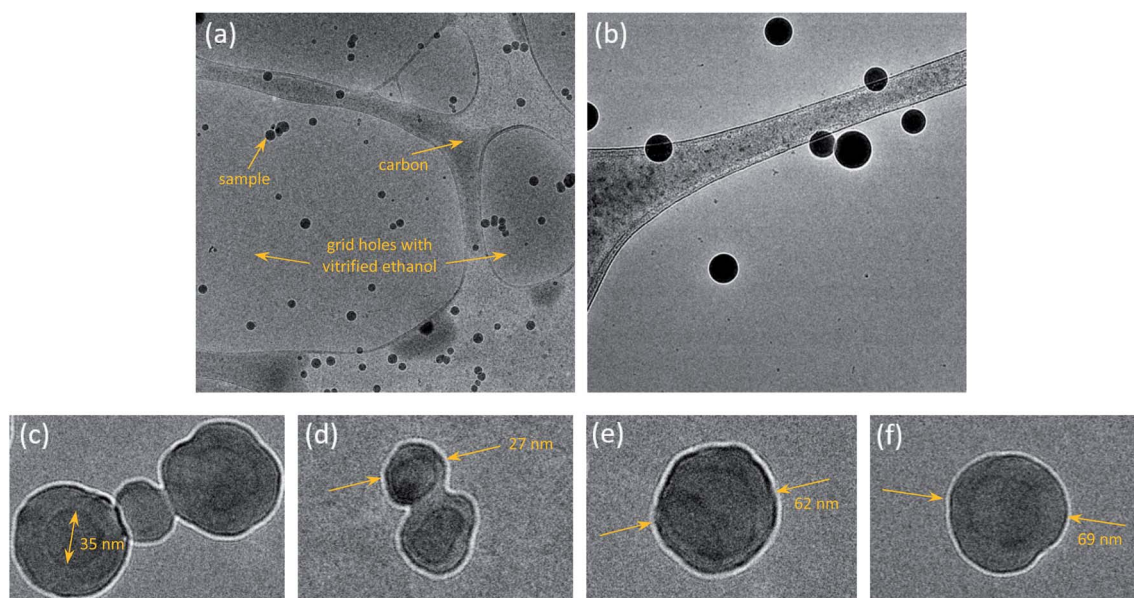
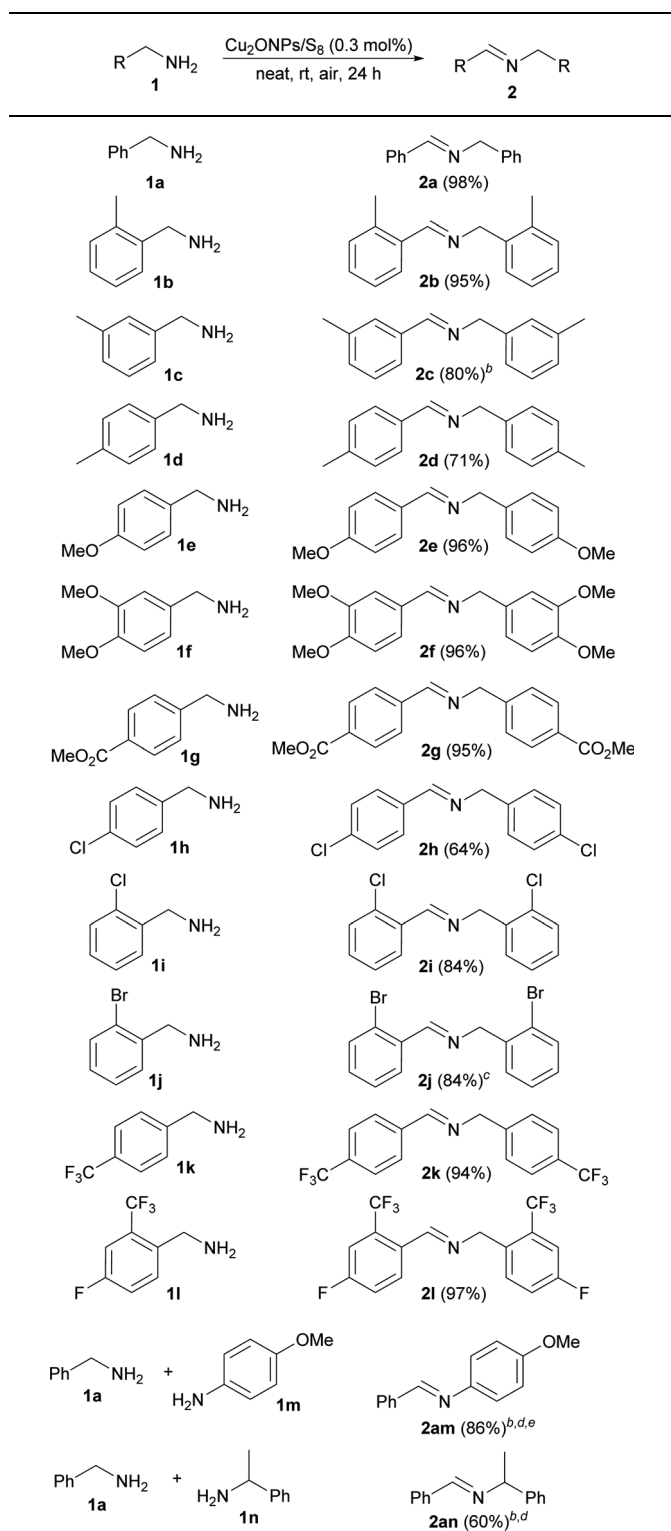


Fig. 6 Cryo-EM images of $\text{Cu}_2\text{ONPs/S}_8$ on carbon grids in ethanol at (a) 17 500 \times , (b) 45 000 \times , and (c)–(f) 150 000 \times .

Table 2 Aerobic oxidation of amines **1** to imines **2**^a

^a Reaction conditions: amine (**1**, 1.0 mmol), Cu₂ONPs/S₈ (0.3 mol%), neat, rt, air, 24 h; isolated yield in parentheses after filtration and solvent evaporation or recrystallisation from hexane, unless otherwise stated. ^b Isolated yield after column chromatography (basic alumina, hexane-EtOAc). ^c From **1j**·HCl in the presence of Et₃N (1.0 mmol). ^d 1 : 3 molar ratio **1a**/**1m,n**. ^e Reaction at 50 °C.

as a stabilising agent, maintaining a small nanoparticle size and preventing their agglomeration.

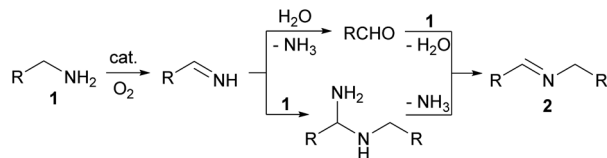
Substrate scope

The applicability of Cu₂ONPs/S₈ to a variety of primary amines was then explored at room temperature under solvent-free conditions in air (Table 2). Both benzylamine (**1a**) and the three regiosomeric (tolylmethyl)amines (**1b–1d**) were transformed into the corresponding imines in >95% conversion and good-to-excellent isolated yields. Very high isolated yields were recorded for the methoxy-, dimethoxy- and methoxycarbonyl-substituted imines **2e**, **2f**, and **2g**, respectively. The standard conditions applied to the chlorinated (**1h** and **1i**) and brominated benzylamines (**1j**) led to the expected imines (**2h–2j**) in nearly quantitative conversion (>96%) and moderate-to-good yields after recrystallisation. The method was equally efficient for the fluorinated benzylamines **1k** and **1l**. It is known that heterocoupled imines by this approach are much less accessible due to the intrinsic self-coupling properties of the substrate. Interestingly, the oxidative heterocondensation of amines catalysed by Cu₂ONPs/S₈ was plausible by using an excess of one of the amines (1 : 3 molar ratio). For instance, benzylamine (**1a**) was successfully coupled with 4-methoxyaniline (**1m**); a gentle warming was helpful to obtain the benzylideneaniline **2am** in high isolated yield. In another example, the reaction of benzylamine (**1a**) with α-methylbenzylamine (**1n**) gave the imine **2an** in moderate isolated yield as a single isomer. The exclusive formation of the C=N double bond on the unsubstituted benzylamine moiety suggests that the unsubstituted benzylamine **1a** is more easily oxidised than the substituted benzylamine **1n**, something that could be due to the more steric hindrance of the latter when interacting with the catalyst.

It is worthy of note that, given the excellent conversions generally attained, most of the reactions required a simple filtration and solvent evaporation work-up or crystallisation of the product in hexane. This procedural simplification is particularly advantageous when taking into account the sensitivity of imines towards hydrolysis. In a few cases (Table 2, **2c**, **2am** and **2an**), column chromatography on basic alumina is recommended to purify the product from small amounts of aldehyde and/or starting material. Purification of **2f** was troublesome, given its susceptibility to hydrolysis; the product could be successfully purified by bulb-to-bulb distillation. In addition, although primary amines may also lead to nitrile, amide, or azo compounds under oxidising conditions, these by-products were not detected because of the very mild reaction conditions applied, leading to a high selectivity towards the imines.

Reaction mechanism

Detailed studies on the reaction mechanism of the catalytic oxidation of primary amines to imines are scarce.¹⁸ A major challenge is to ascertain whether the reaction involves an aldehyde intermediate, formed by the dehydrogenation of the primary amine and further hydrolysis of the resulting imine (Scheme 3, path A), or only the primary amine (Scheme 3, path B).



Scheme 3 Generally accepted possible routes in the catalytic aerobic oxidation of primary amines (1) to imines (2).

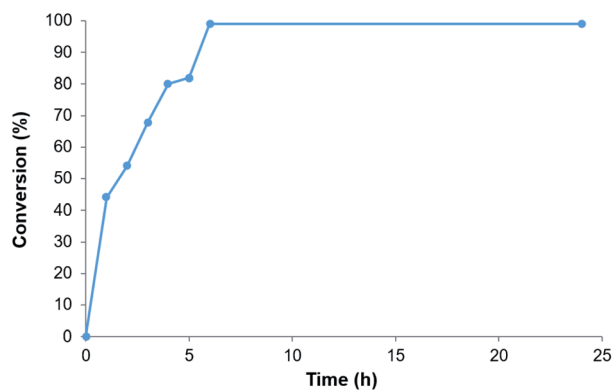
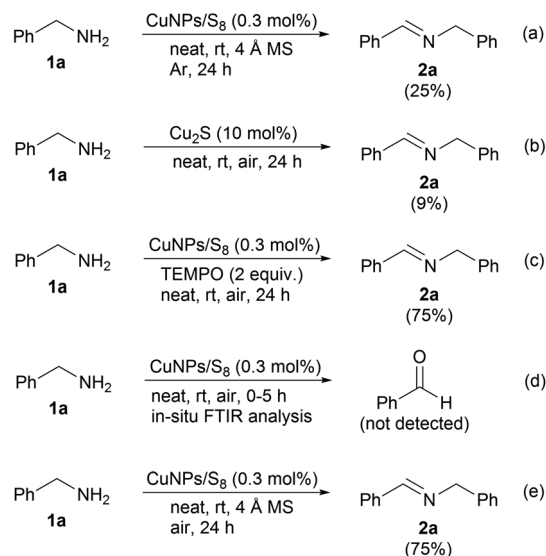


Fig. 7 Reaction profile in the aerobic oxidation of benzylamine (1a) to the imine 2a.

We carried out a series of experiments in order to shed light on the reaction mechanism. However, first, the kinetic profile for the aerobic oxidation of benzylamine (1a) to benzylidenebenzylamine (2a) was recorded. As depicted in Fig. 7, nearly half conversion is reached in the first hour, with the reaction being complete after 6 h. The intermediate aldehyde was not detected in any of the samples analysed by GLC or GC-MS.

The standard reaction of benzylamine, when conducted under anaerobic and anhydrous conditions led to only 25% of the expected imine (Scheme 4a); this result is in agreement with



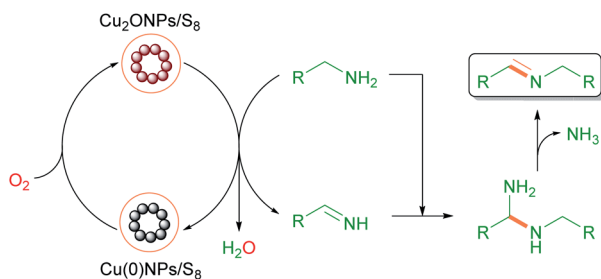
Scheme 4 Experiments to support the reaction mechanism.

the control experiment in Table 1 (entry 17) where, apparently, the reaction is promoted to some extent by the solely action of S₈, which likely dehydrogenates the substrate to give species of the type H₂S_x. This hypothesis is supported by the fact that a red-coloured stuff (typical of polysulfides or polymeric sulfur)³⁷ was observed at the end of the reactions, accompanied by a smell resembling that of H₂S. In order to rule out any possible formation of copper sulfides (e.g., Cu₂S or Cu polysulfides) that could catalyse the reaction, an experiment with commercial copper(i) sulfide (10 mol% Cu₂S) was conducted under the standard conditions (Scheme 4b). The conversion into the expected product was found to be 9%. Therefore, we can conclude that the probability of formation of copper sulfides in the reaction medium that might catalyse the reaction is very low.

The addition of an excess of the radical trap TEMPO to the reaction mixture did not substantially inhibit the reaction and no TEMPO-radical adducts were detected, practically ruling out the participation of free-radical species (Scheme 4c). We also monitored a reaction by *in situ* FTIR analysis in the search for benzaldehyde as a potential reaction intermediate (Scheme 4d); however, this compound was not detected. In another experiment, 4 Å molecular sieves were added to the reaction medium with the aim to trap any water released from the amine oxidation step (Scheme 4e); under these conditions, low product yield would be expected if the aldehyde were formed by the primary imine hydrolysis and further condensed with another equivalent of the amine (1a) to give the imine 2a. Quite the opposite, the imine 2a was obtained in good yield (Scheme 4e), though not quantitative because the solid molecular sieves could interfere somewhat in the reaction due to the neat conditions applied. Therefore, from these experiments we can conclude that (a) the presence of Cu and oxygen (from air) are mandatory to attain high conversions, though a background reaction with S₈ might be occurring at the same time to a much lower extent; (b) the reaction takes place through an ionic pathway; and (c) aldehydes do not participate as reaction intermediates.

It is worthwhile mentioning that, when recovered after use, the catalyst showed a similar XPS spectrum to that of the fresh catalyst, with two peaks at binding energies of 932.1 and 933.7 eV (ESI, Fig. S7†). This fact, together with the absence of the satellite peaks typical of CuO, points to a mechanism operating through Cu₂O and Cu⁰ species. Indeed, the groups of Adimurthy,³⁸ and Cao and Gu^{22c} independently reported the use of Cu⁰ in the title reaction, where *in situ* formed Cu^I is the catalytically active species. In particular, the group of Adimurthy used Cu⁰ powder at 90 °C in air for 20 h; Cu⁰ powder can contain Cu₂O on the surface if not subjected to any previous treatment, but even if pure Cu⁰ would be used, the formation of Cu₂O in the reaction medium would be expected after heating to such temperature and time in air. Similarly, Cao and Gu utilised red Cu at 100 °C under 1 atm of O₂ for 24 h, conditions that must readily promote the oxidation of Cu⁰ to Cu₂O.

On the basis of the aforementioned information, a reaction mechanism was proposed (Scheme 5), involving: (a) the oxidation of the starting amine to the corresponding primary imine catalysed by Cu₂ONPs/S₈, with the concomitant formation of



Scheme 5 Proposed reaction mechanism.

water and Cu(0)NPs/S₈; (b) the addition of a second molecule of amine to the C=N bond of the primary imine to give an aminal; (c) the release of ammonia from the aminal to give the imine product; and (d) the regeneration of Cu₂ONPs/S₈ under the action of O₂. It is worth noting that the release of ammonia from the reaction tubes was very evident by olfactory detection.

Comparison with commercial catalysts

Finally, we compared the catalytic activity of Cu₂ONPs/S₈ with that of a range of commercial copper catalysts. For this purpose, 0.3 mol% Cu₂ONPs/S₈ and 1–10 mol% Cu loading for the rest of the commercial catalyst were applied at room temperature, under air and solvent-free conditions.

It can be concluded from Table 3 that (a) the commercial catalysts Cu, CuI, CuBr·SMe₂, CuBr₂, CuCl, CuCl₂, CuOAc, Cu(OAc)₂, CuOTf and Cu(OTf)₂ at 10 mol% led to the imine **2a** in conversions ≤30% (Table 3, entries 1–10); (b) the commercial

Table 3 Screening of different Cu catalysts in the oxidation of benzylamine (**1a**)^a

Entry	Catalyst	mol%	Conversion ^b (%)
1	Cu(0)	10	13
2	CuI	10	15
3	CuBr·SMe ₂	10	24
4	CuBr ₂	10	2
5	CuCl	10	30
6	CuCl ₂	10	2
7	CuOAc	10	5
8	Cu(OAc) ₂	10	3
9	CuOTf	10	9
10	Cu(OTf) ₂	10	15
11	CuO	10	6
12	Cu ₂ O	10	82
13	Cu ₂ O	5	32
14	Cu ₂ O	1	5
15	Cu ₂ O + S ₈	10 ^c	71
16	Cu ₂ S	10	9
17	Cu ₂ ONPs/S ₈	0.3	>99

^a Reaction conditions: **1a** (1 mmol), Cu catalyst, neat, air, rt, 24 h.

^b Conversion into **2a** determined by GLC. ^c Cu₂O (10 mol%) + S₈ (10 mol%).

Cu(I) catalysts generally perform much better than the Cu(II) catalysts [CuBr·SMe (24%), Cu₂Br (2%); CuCl (30%), CuCl₂ (2%); CuOAc (5%), Cu(OAc)₂ (3%); Cu₂O (82%), CuO (6%)]; and (c) the commercial Cu(I) oxide performs much better than any of the Cu(I) salts. Therefore, the oxidation state (I) and the presence of oxygen in the catalyst seem to be very important factors for successful catalytic activity. The highest conversion attained with Cu₂O (10 mol%) is in concordance with the performance and composition of our catalyst (*i.e.*, Cu₂ONPs/S₈) (Table 3, compare entries 12 and 17). However, a substantial decrease in the conversion was noticed when the Cu₂O loading was reduced to 5 and 1 mol% (Table 3, entries 13 and 14, respectively). A possible co-catalytic effect between Cu₂O and sulfur was ruled out as when added together (10 mol% each) the conversion was lower than with Cu₂O alone (Table 3, compare entries 12 and 15). Commercial Cu₂S proved inefficient, practically discarding any possible formation of Cu₂S during the catalyst preparation or during the amine reaction (Table 3, entry 16). Therefore, the nanostructured character of copper, combined with the stabilising effect of sulfur, seem to be crucial for the outstanding catalytic activity of Cu₂ONPs/S₈, reaching quantitative conversion with low metal loading (Table 3, entry 17).

Conclusions

It has been demonstrated that very abundant and inexpensive elemental sulfur is an adequate stabilisation agent for CuNPs, in the form of copper(I) oxide, preventing their agglomeration and over-oxidation for years. It is remarkable that, in organic medium, nanodroplets of Cu₂ONPs/S₈ are formed, where the Cu₂ONPs are assembled as concentric nanorings inside a spherical matrix of sulfur. Cu₂ONPs/S₈ has been shown to effectively catalyse the oxidation of benzylic primary amines at very low loading (0.3 mol%) under solvent-free conditions, at room temperature and using the molecular oxygen of air as a terminal oxidant. The method is applicable to both the homo- and heterocoupling of amines, furnishing the imines in moderate-to-excellent yields (60–98%). A reaction mechanism has been proposed, based on experimentation, where the participation of intermediate aldehydes has been ruled out and where the Cu⁰–Cu^I pair seems to be operating in the catalytic cycle. Moreover, Cu₂ONPs/S₈ exhibits a salient performance when compared with a range of commercial Cu catalysts. The simplicity of the catalytic system provides a cheaper, less toxic and more effective alternative to processes that have previously required expensive catalysts, including those based on iridium, ruthenium, palladium and gold. Furthermore, the findings described herein can pave the way for research on the stabilisation and catalytic applications of other metal nanoparticles.

Experimental

General procedure for the preparation of CuNPs/support

Dry THF (2 mL) was added dropwise to a mixture of lithium powder (14 mg, 2.0 mmol) and 4,4'-di-*tert*-butylbiphenyl (DTBB, 27 mg, 0.1 mmol), under an argon atmosphere. Anhydrous CuCl₂ (134 mg, 1.0 mmol) was then added to the green

suspension, which rapidly turned black upon the formation of CuNPs. This suspension was diluted with THF (18 mL), followed by the addition of the corresponding support (1.28 g). The resulting mixture was stirred for 1 h at room temperature, filtered, and the solid was successively washed with THF (20 mL) and MeOH (20 mL), and dried under vacuum.

General procedure for the preparation of Cu₂ONPs/S₈

Anhydrous CuCl₂ (134 mg, 1.0 mmol) was dissolved in absolute EtOH (15 mL) and S₈ (1.28 g) was added to the resulting solution. The mixture was stirred, followed by the addition of NaBH₄ (4 equiv.). The resulting mixture was stirred for 1 h at rt, filtered, and the solid was successively washed with water (20 mL), EtOH (10 mL) and THF (10 mL), and dried under vacuum.

General procedure for the aerobic oxidation of amines

The amine **1** (1.0 mmol) was added to a reactor tube containing Cu₂ONPs/S₈ (20 mg, 0.3 mol%) and the mixture was stirred at room temperature for 24 h without any solvent. The resulting mixture was diluted with EtOAc, filtered through a pad of neutral alumina, celite and MgSO₄, and the filtrate was analysed by GLC and GC-MS and concentrated under vacuum. The imines **2** were generally purified by recrystallisation from hexane. Imines **2a**, **2g** and **2l** were obtained in quantitative conversion and did not require any further purification; imines **2c**, **2am** and **2an** were purified by column chromatography (basic alumina, hexane-EtOAc); the very sensitive imine **2f** was purified by bulb-to-bulb distillation under vacuum.

Conflicts of interest

There are no conflicts to declare.

Acknowledgements

This work was generously supported by the Spanish Ministerio de Ciencia, Innovación y Universidades (MICIU; grant no. CTQ2017-88171-P), the Generalitat Valenciana (GV; grant no. AICO/2017/007), and the Instituto de Síntesis Orgánica (ISO). I. M.-G. thanks the Vicerrectorado de Investigación y Transferencia del Conocimiento of the Universidad de Alicante for a pre-doctoral grant (no. UAFPU2016-034). G. S. is grateful to the European Union for an Erasmus grant. Y. M. thanks the ISO for a postdoctoral grant. We also acknowledge M. C. Román-Martínez for her advice on the nitrogen isotherm and the CNB-CIB (CSIC) (Rocío Arranz and M. Teresa Bueno-Carrasco) for its technical advice and support on the CryoEM facility.

Notes and references

- 1 Selected monographs: (a) *Metal Nanoclusters in Catalysis and Material Science. The Issue of Size Control*, ed. B. Corain, G. Schmid and N. Toshima, Elsevier, Amsterdam, 2008; (b) *Nanoparticles and Catalysis*, ed. D. Astruc, Wiley-VCH, Weinheim, 2008; (c) *Selective Nanocatalysts and Nanoscience*, ed. A. Zecchina, S. Bordiga and E. Groppo,

Wiley-VCH, Weinheim, 2011; (d) *Nanocatalysis. Synthesis and Applications*, ed. V. Polshettiwar and T. Asefa, Wiley-VCH, Weinheim, 2013; (e) *Metal Nanoparticles for Catalysis: Advances and Applications*, ed. F. Tao, The Royal Society of Chemistry, Cambridge (UK), 2014.

- 2 Selected reviews: (a) A. Roucoux, J. Schulz and H. Patin, Reduced transition metal colloids: a novel family of reusable catalysts?, *Chem. Rev.*, 2002, **102**, 3757–3778; (b) T. Cheng, D. Zhang, H. Li and G. Li, Magnetically recoverable nanoparticles as efficient catalysts for organic transformations in aqueous medium, *Green Chem.*, 2014, **16**, 3401–3427; (c) C. Xu, S. De, A. M. Balu, M. Ojeda and R. Luque, Mechanochemical synthesis of advanced nanomaterials for catalytic applications, *Chem. Commun.*, 2015, **51**, 6698–6713; (d) R. Ricciardi, J. Huskens and W. Verboom, Nanocatalysis in Flow, *ChemSusChem*, 2015, **8**, 2586–2605; (e) L. Chen and Y. Li, Heterogeneous room temperature catalysis-nanomaterials, in *Sustainable Catalysis. Energy-Efficient Reactions and Applications*, ed. R. Luque and F. L.-Y. Lam, Wiley-VCH, Weinheim, 2018, ch. 3, pp. 59–87; (f) J. M. Asensio, D. Bouzouita, P. W. N. M. van Leeuwen and B. Chaudret, σ -H–H, σ -C–H, and σ -Si–H Bond activation catalyzed by metal nanoparticles, *Chem. Rev.*, 2020, **120**, 1042–1084.
- 3 (a) *Inorganic Nanoparticles: Synthesis, Applications and Perspectives*, ed. C. Altavilla and E. Ciliberto, CRC Press, London, 2010; (b) Review: K. An, S. Alayoglu, T. Ewers and G. Somorjai, Colloid chemistry of nanocatalysts: a molecular view, *J. Colloid Interface Sci.*, 2012, **373**, 1–13; (c) *Nanoparticles: From Theory to Application*, ed. G. Schmid, Wiley-VCH, Weinheim, 2nd edn, 2010; (d) H. Goesmann and C. Feldmann, Nanoparticulate functional materials, *Angew. Chem., Int. Ed.*, 2010, **49**, 1362–1395; (e) D. Vollath, *Nanomaterials: An Introduction to Synthesis, Properties and Applications*, Wiley-VCH, Weinheim, 2nd edn, 2013.
- 4 M. B. Gawande, A. Goswami, F.-X. Felpin, T. Asefa, X. Huang, R. Silva, X. Zou, R. Zboril and R. S. Varma, Cu and Cu-based nanoparticles: synthesis and applications in catalysis, *Chem. Rev.*, 2016, **116**, 3722–3811.
- 5 S. E. Allen, R. R. Walvoord, R. Padilla-Salinas and M. C. Kozlowski, Aerobic copper-catalyzed organic reactions, *Chem. Rev.*, 2013, **113**, 6234–6458.
- 6 See, for instance: (a) A. Yabuki and S. Tanaka, Oxidation behaviour of copper nanoparticles at low temperature, *Mater. Res. Bull.*, 2011, **46**, 2323–2327; (b) M. Alsawaf, S. Badilescu, M. Packirisamy and V.-V. Truong, Kinetics at the nanoscale: formation and aqueous oxidation of copper nanoparticles, *React. Kinet., Mech. Catal.*, 2011, **104**, 437–450; (c) N. L. Pacioni, V. Filippenko, N. Presseau and J. C. Scaiano, Oxidation of copper nanoparticles in water: mechanistic insights revealed by oxygen uptake and spectroscopic methods, *Dalton Trans.*, 2013, **42**, 5832–5838; (d) G. Zhou, L. Luo, L. Li, J. Ciston, E. A. Stach, W. A. Saidi and J. C. Yang, In situ atomic-scale visualization of oxide islanding during oxidation of Cu surfaces, *Chem. Commun.*, 2013, **49**, 10862–10864; (e) A. P. LaGrow, M. R. Ward, D. C. Lloyd, P. L. Gai and E. D. Boyes, Visualizing the Cu/

- Cu₂O interface transition in nanoparticles with environmental scanning transmission electron microscopy, *J. Am. Chem. Soc.*, 2017, **138**, 179–185.
- 7 See, for instance: (a) M. Xiaopeng, J. Wen, Y. Yao, Y. Ding, Y. Gong, C. Zou, G. Yin, X. Liao, Z. Huang and X. Chen, A facile synthesis of monodispersed carbon-encapsulated copper nanoparticles with excellent oxidation resistance from a refluxing-derived precursor, *Chem. Lett.*, 2013, **42**, 627–629; (b) P. Abdulkin, Y. Moglie, B. R. Knappett, D. A. Jefferson, M. Yus, F. Alonso and A. E. H. Wheatley, New routes to Cu(I)/Cu nanocatalysts for the multicomponent click synthesis of 1,2,3-triazoles, *Nanoscale*, 2013, **5**, 342–350; (c) M. Nishida and T. Tsukuda, Production of oxidation-resistant copper nanoparticles on carbon nanotubes by photoreduction, *Chem. Lett.*, 2013, **46**, 168–170.
- 8 (a) Spotlight: J. S. Bello Forero, Elemental sulphur: a simple, economic, and versatile reagent, *Synlett*, 2011, 1786–1787; (b) Review: H. Liu and X. Jiang, Transfer of sulphur: from simple to diverse, *Chem.-Asian J.*, 2013, **8**, 2546–2563; (c) Q. Zu, S. L. Wegener, C. Xie, O. Uche, M. Neurock and T. J. Marks, Sulfur as a selective ‘soft’ oxidant for catalytic methane conversion proved by experiment and theory, *Nat. Chem.*, 2013, **5**, 104–109; (d) Review: T. B. Nguyen, Recent advances in organic reactions involving elemental sulfur, *Adv. Synth. Catal.*, 2017, **359**, 1066–1130.
- 9 (a) W. J. Chung, J. J. Griebel, E. T. Kim, H. Yoon, A. G. Simmonds, H. J. Ji, P. T. Dirlam, R. S. Glass, J. J. Wie, N. A. Nguyen, B. W. Guralnick, J. Park, A. Somogy, P. Theato, M. E. Mackay, Y.-E. Sung, K. Char and J. Pyun, The use of elemental sulfur as an alternative feedstock for polymeric materials, *Nat. Chem.*, 2013, **5**, 518–524; (b) Minireview: J. Lim, J. Pyun and K. Char, Recent approaches for the direct use of elemental sulfur in the synthesis and processing of advanced materials, *Angew. Chem., Int. Ed.*, 2015, **54**, 3249–3258; (c) S. H. He, O. Buyukcakir, D. Kim and A. Coskun, Direct utilization of elemental sulfur in the synthesis of microporous polymers for natural gas sweetening, *Chem*, 2016, **1**, 482–493; (d) L. Peng, Z. Wei, C. Wan, J. Li, Z. Chen, D. Zhu, D. Baumann, H. Liu, C. S. Allen, X. Xu, A. I. Kirkland, I. Shakir, Z. Almutairi, S. Tolbert, B. Dunn, Y. Huang, P. Sautet and X. Duan, A fundamental look at electrocatalytic sulfur reduction reaction, *Nat. Catal.*, 2020, **3**, 762–770.
- 10 W. J. Chung, A. G. Simmonds, J. J. Griebel, E. T. Kim, H. S. Suh, I.-B. Shim, R. S. Glass, D. A. Loy, P. Theato, Y.-E. Sung, K. Char and J. Pyun, Elemental sulfur as a reactive medium for gold nanoparticles and nanocomposite materials, *Angew. Chem., Int. Ed.*, 2011, **50**, 11409–11412.
- 11 Reviews: (a) S. Goel, F. Chen and W. Cai, Synthesis and biomedical applications of copper sulfide nanoparticles: from sensors to theranostics, *Small*, 2014, **10**, 631–645; (b) L. Wang, Synthetic methods of CuS nanoparticles and their applications for imaging and cancer therapy, *RSC Adv.*, 2016, **6**, 82596–82615; (c) Y. Liu, J. Yang and P. Wang, Recent advances in small copper sulfide nanoparticles for molecular imaging and tumor therapy molecular pharmaceuticals, *Mol. Pharmaceutics*, 2019, **16**, 3322–3332; (d) See also: T.-T. Zhuang, Z.-Q. Liang, A. Seifitokaldani, Y. Li, P. De Luna, T. Burdyny, F. Che, F. Meng, Y. Min, R. Quintero-Bermudez, C. T. Dinh, Y. Pang, M. Zhong, B. Zhang, J. Li, P.-N. Chen, X.-L. Zheng, H. Liang, W.-N. Ge, B.-J. Ye, D. Sinton, S.-H. Yu and E. H. Sargent, Steering post-C-C coupling selectivity enables high efficiency electroreduction of carbon dioxide to multi-carbon alcohols, *Nat. Catal.*, 2018, **1**, 421–428.
- 12 General review: J. Adams, Imines, enamines and oximes, *J. Chem. Soc., Perkin Trans. 1*, 2000, 125–139.
- 13 Recent reviews: (a) J.-D. Yang, J. Xue and J.-P. Cheng, Understanding the role of thermodynamics in catalytic imine reductions, *Chem. Soc. Rev.*, 2019, **48**, 2913–2926; (b) R. Innocenti, E. Lenci and A. Trabocchi, Recent advances in copper-catalyzed imine-based multicomponent reactions, *Tetrahedron Lett.*, 2020, **61**, 152083; (c) K. Morisaki, H. Morimoto and T. Ohshima, Recent progress on catalytic addition reactions to N-unsubstituted imines, *ACS Catal.*, 2020, **10**, 6924–6951; (d) T.-C. Chang, A. R. Pradipta and K. Tanaka, Enantioselective synthesis of cyclic and linear diamines by imine cycloadditions, *Chirality*, 2020, **32**, 1160–1168.
- 14 See, for instance the reviews: (a) M. Albrecht and I. Janser, Catechol imine ligands: from helicates to supramolecular tetrahedra, *Chem. Commun.*, 2005, 157–165; (b) N. F. Curtis, Syntheses and structures of compounds with acyclic imine ligands formed by reactions of coordinated amines with carbonyl compounds, *Inorg. Chim. Acta*, 2019, **498**, 118843.
- 15 (a) H. Schiff, Mittheilungen aus dem universitätslaboratorium in Pisa: eine neue reihe organischer basen, *Ann. Chem.*, 1864, **131**, 118–119; (b) L. J. Silverberg, D. J. Coyle, K. C. Cannon, R. J. Mathers, J. A. Richards and J. Thierney, Azeotropic preparation of a C-phenyl N-aryl imine: an introductory undergraduate organic chemistry laboratory experiment, *J. Chem. Educ.*, 2016, **93**, 941–944.
- 16 Reviews: (a) T. D. Nixon, M. K. Whittlesey and J. M. J. Williams, Transition metal catalysed reactions of alcohols using borrowing hydrogen methodology, *Dalton Trans.*, 2009, 753–762; (b) S. Bähn, S. Imm, L. Neubert, M. Zhang, H. Neumann and M. Beller, The catalytic amination of alcohols, *ChemCatChem*, 2011, **3**, 1853–1864; (c) Y. Obora, Recent advances in α -alkylation reactions using alcohols with hydrogen borrowing methodologies, *ACS Catal.*, 2014, **4**, 3972–3981; (d) M. N. Kopylovich, A. P. Ribeiro, E. C. Alegria, N. M. Martins, L. M. Martins and A. J. Pombeiro, Catalytic oxidation of alcohols: Recent advances, *Adv. Organomet. Chem.*, 2015, **63**, 91–174.
- 17 See, for instance: (a) B. Zhu and R. J. Angelici, Non-nanogold catalyzed aerobic oxidation of secondary amines to imines, *Chem. Commun.*, 2007, 2157–2159; (b) M.-H. So, Y. Liu, C.-M. Ho and C.-M. Che, Graphite-supported gold nanoparticles as efficient catalyst for aerobic oxidation of benzylic amines to imines and N-substituted 1,2,3,4-

- tetrahydroisoquinolines to amides: synthetic applications and mechanistic study, *Chem.-Asian J.*, 2009, **4**, 1551–1561; (c) H. Miyamura, M. Morita, T. Inasaki and A. Kobayashi, Aerobic oxidation of amines by polymer-incarcerated Au nanoclusters: effect of cluster size and cooperative functional groups in the polymer, *Bull. Chem. Soc. Jpn.*, 2011, **84**, 588–599; (d) H. Yuan, W.-J. Yoo, H. Miyamura and S. Kobayashi, Discovery of a metalloenzyme-like cooperative catalytic system of metal nanoclusters and catechol derivatives for the aerobic oxidation of amines, *J. Am. Chem. Soc.*, 2012, **134**, 13970–13973.
- 18 Reviews: (a) M. Langeron, Protocols for the catalytic oxidation of primary amines to imines, *Eur. J. Org. Chem.*, 2013, 5225–5235; (b) B. Chen, L. Wang and S. Gao, Recent advances in aerobic oxidation of alcohols and amines to imines, *ACS Catal.*, 2015, **5**, 5851–5876.
- 19 See, for instance: (a) B. Zhu, M. Lazar, B. G. Trewyn and R. J. Angelici, Aerobic oxidation of amines to imines catalyzed by bulk gold powder and by alumina-supported gold, *J. Catal.*, 2008, **260**, 1–6; (b) A. Girrane, A. Corma and H. Garcia, Highly active and selective gold catalysts for the aerobic oxidative condensation of benzylamines to imines and one-pot, two-step synthesis of secondary benzylamines, *J. Catal.*, 2009, **264**, 138–144.
- 20 A. Prades, E. Peris and M. Albrecht, Oxidations and oxidative couplings by triazolylidene ruthenium complexes, *Organometallics*, 2011, **30**, 1162–1167.
- 21 C. Hammond, M. T. Schümperli and I. Hermans, Insights into the oxidative dehydrogenation of amines with nanoparticulate iridium oxide, *Chem.-Eur. J.*, 2013, **19**, 13193–13198.
- 22 See, for instance: (a) R. D. Patil and S. Adimurthy, Copper-catalyzed aerobic oxidation of amines to imines under neat conditions with low catalyst loading, *Adv. Synth. Catal.*, 2011, **353**, 1695–1700; (b) M. Langeron and M.-B. Fleury, A biologically inspired Cu^I/topaquinone-like co-catalytic system for the highly atom-economical aerobic oxidation of primary amines to imines, *Angew. Chem., Int. Ed.*, 2012, **51**, 5409–5412; (c) J. Wang, S. Lu, X. Cao and H. Gu, Common metal of copper(0) as an efficient catalyst for preparation of nitriles and imines by controlling additives, *Chem. Commun.*, 2014, **50**, 5637–5640; (d) M. Langeron and M.-B. Fleury, A metalloenzyme-like catalytic system for the chemoselective oxidative cross-coupling of primary amines to imines under ambient conditions, *Chem.-Eur. J.*, 2015, **21**, 3815–3820; (e) A. T. Murray, R. King, J. V. G. Donnelly, M. J. H. Dowley, F. Tuna, D. Sells, M. P. John and D. R. Carbery, Symbiotic transition-metal and organocatalysis for catalytic ambient amine oxidation and alkene reduction reactions, *ChemCatChem*, 2016, **8**, 510–514.
- 23 (a) F. Bottaro, A. Takallou, A. Chehaiber and R. Madsen, Cobalt-catalyzed dehydrogenative coupling of amines into imines, *Eur. J. Org. Chem.*, 2019, 7164–7168; (b) X. Cui, W. Li, K. Junge, Z. Fei, M. Beller and P. J. Dyson, Selective acceptorless dehydrogenation of primary amines to imines by core-shell cobalt nanoparticles, *Angew. Chem., Int. Ed.*, 2020, **132**, 7571–7577.
- 24 (a) Z. Zhang, F. Wang, M. Wang, S. Xu, H. Chen, C. Zhang and J. Xu, *tert*-Butyl hydroperoxide (TBHP)-mediated oxidative self-coupling of amines to imines over a α -MnO₂ catalyst, *Green Chem.*, 2014, **16**, 2523–2527; (b) S. Biswas, B. Dutta, K. Mullick, C.-H. Kuo, A. S. Poyraz and S. L. Suib, Aerobic oxidation of amines to imines by cesium-promoted mesoporous manganese oxide, *ACS Catal.*, 2015, **5**, 4394–4403.
- 25 G. Jaiswall, V. G. Landge, D. Jagadeesan and E. Balaraman, Iron-based nanocatalyst for the acceptorless dehydrogenation reactions, *Nat. Commun.*, 2017, **8**, 2147.
- 26 See, for instance: (a) L. Liu, S. Zhang, X. Fu and C. Yan, Metal-free aerobic oxidative coupling of amines to imines, *Chem. Commun.*, 2011, **47**, 10148–10150; (b) H. Huang, J. Huang, Y.-M. Liu, H.-Y. He, Y. Cao and K.-N. Fan, Graphite oxide as an efficient and durable metal-free catalyst for aerobic oxidative coupling of amines to imines, *Green Chem.*, 2012, **14**, 930–934; (c) A. Monopoli, P. Cotugno, F. Iannone, F. Ciminale, M. M. Dell'Anna, P. Mastrorilli and A. Nacci, Ionic-liquid-assisted metal-free oxidative coupling of amines to give imines, *Eur. J. Org. Chem.*, 2014, 5925–5931.
- 27 See, for instance: (a) X. Lang, H. Ji, C. Chen, W. Ma and J. Zhao, Selective formation of imines by aerobic photocatalytic oxidation of amines on TiO₂, *Angew. Chem., Int. Ed.*, 2011, **50**, 3934–3937; (b) F. Su, S. C. Mathew, L. Möhlmann, M. Antonietti, X. Wang and S. Blechert, Aerobic oxidative coupling of amines by carbon nitride photocatalysis with visible light, *Angew. Chem., Int. Ed.*, 2011, **50**, 657–660; (c) M. Rueping, C. Vila, A. Szadkowska, R. M. Koenigs and J. Fronert, Photoredox catalysis as an efficient tool for the aerobic oxidation of amines and alcohols: bioinspired demethylation and condensations, *ACS Catal.*, 2012, **2**, 2810–2815; (d) L.-N. Unkel, S. Malcherek, E. Schendera, F. Hoffmann, J. Rehbein and M. Brasholz, Photoorganocatalytic aerobic oxidative amine dehydrogenation/super acid-mediated Pictet-Spengler cyclization: synthesis of *cis*-1,3-diaryl tetrahydroisoquinolines, *Adv. Synth. Catal.*, 2019, **361**, 2870–2876; (e) Y. Xiao, G. Tian, W. Li, Y. Xie, B. Jiang, C. Tian, D. Zhao and H. Fu, Molecule self-assembly synthesis of porous few-layer carbon nitride for highly efficient photoredox catalysis, *J. Am. Chem. Soc.*, 2019, **141**, 2508–2515.
- 28 For a former account, see: F. Alonso and M. Yus, New synthetic methodologies based on active transition metals, *Pure Appl. Chem.*, 2008, **80**, 1005–1012.
- 29 F. Alonso, J. J. Calvino, I. Osante and M. Yus, A new straightforward and mild preparation of nickel(0) nanoparticles, *Chem. Lett.*, 2005, **34**, 1262–1263.
- 30 Recent applications of supported CuNPs from our group: (a) F. Alonso, A. Arroyo, I. Martín-García and Y. Moglie, Cross-dehydrogenative coupling of tertiary amines and terminal alkynes catalyzed by copper nanoparticles on zeolite, *Adv. Synth. Catal.*, 2015, **357**, 3549–3561; (b) A. Y. Mitrofanov, A. V. Murashkina, I. Martín-García, F. Alonso and I. P. Beletskaya, Formation of C-C, C-S and C-N bonds

- catalysed by supported copper nanoparticles, *Catal. Sci. Technol.*, 2017, 7, 4401–4412; (c) I. Martín-García and F. Alonso, Synthesis of dihydroindoloisoquinolines through the copper-catalyzed cross-dehydrogenative coupling of tetrahydroisoquinolines and nitroalkanes, *Chem.–Eur. J.*, 2018, 24, 18857–18862.
- 31 For an application of elemental sulfur in the multicomponent synthesis of thioamides from aliphatic amines, see: T. B. Nguyen, L. Ermolenko and A. Al-Mourabit, Efficient and selective multicomponent oxidative coupling of two different aliphatic amines into thioamides by elemental sulfur, *Org. Lett.*, 2012, 14, 4274–4277.
- 32 Reviews: (a) M. Thommes, K. Kaneko, A. V. Neimark, J. P. Olivier, F. Rodriguez-Reinoso, J. Rouquerol and K. S. W. Sing, Physisorption of gases, with special reference to the evaluation of surface area and pore size distribution (IUPAC Technical Report), *Pure Appl. Chem.*, 2015, 87, 1051–1069; (b) K. S. W. Sing and R. T. Williams, Physisorption hysteresis loops and the characterization of nanoporous materials, *Adsorpt. Sci. Technol.*, 2004, 22, 773–782; (c) See, also: X. Zhang, J. Chen, S. Jiang, X. Zhang, F. Bi, Y. Yang, Y. Wang and Z. Wang, Enhanced photocatalytic degradation of gaseous toluene and liquidus tetracycline by anatase/rutile titanium dioxide with heterophase junction derived from materials of Institut Lavoisier-125(Ti): Degradation pathway and mechanism studies, *J. Colloid Interface Sci.*, 2021, 588, 122–137.
- 33 NIST X-Ray Photoelectron Spectroscopy Database, <https://srdata.nist.gov/xps/>, accessed March 2020.
- 34 I. Nakai, Y. Sugitani, K. Nagashima and Y. Niwa, X-ray photoelectron spectroscopic study of copper minerals, *J. Inorg. Nucl. Chem.*, 1978, 40, 789–791.
- 35 (a) J. C. W. Folmer and F. Jellinek, The valence of copper in sulphides and selenides: an X-ray photoelectron spectroscopy study, *J. Less-Common Met.*, 1980, 76, 153–162; (b) D. L. Perry and J. A. Taylor, X-ray photoelectron and Auger spectroscopic studies of Cu₂S and CuS, *J. Mater. Sci. Lett.*, 1986, 5, 384–386.
- 36 Review: D. Lyumkis, Challenges and opportunities in cryo-EM single-particle analysis, *J. Biol. Chem.*, 2019, 294, 5181–5197.
- 37 J. J. Griebel, R. S. Glass, K. Char and J. Pyun, Polymerizations with elemental sulfur: a novel route to high sulfur content polymers for sustainability, energy and defense, *Prog. Polym. Sci.*, 2016, 58, 90–125.
- 38 R. D. Patil and S. Adimurthy, Copper(0)-catalyzed aerobic oxidative synthesis of imines from amines under solvent-free conditions, *RSC Adv.*, 2012, 2, 5119–5122.